Journal of the European Ceramic Society 16 (1996) 961–973

S0955-2219(96)00012-X
0955-2219/96/$15.00

Sintering Behaviour and Ionic Conductivity of Yttria-Doped Ceria

Jan Van herle,* Teruhisa Horita,† Tatsuya Kawada, Natsuko Sakai, Harumi Yokokawa & Masayuki Dokiya

National Institute of Materials and Chemical Research, 1-1 Higashi, Tsukuba Science City, 305 Ibaraki, Japan

(Received 29 September 1995; revised version received 11 December 1995; accepted 5 January 1996)

Abstract

Highly sinterable yttria-doped ceria powder $(YO_{1.5})_x(CeO_2)_{1-x}$ *(*$x = 0.1$–0.33*) was fabricated by an optimized coprecipitation route. Compacted bodies could be sintered to impermeability at 1200°C and near full density at 1300°C, among the lowest temperatures reported for doped ceria densification. Ceria diffusion is important above 1400°C. Excellent conduction properties were observed: high ionic conductivity (6·5 S* m^{-1} *at 750°C for* $Ce_{0.8}Y_{0.2}O_{1.9}$*), low activation energy (0·7 eV) and vanishing grain-boundary resistance. © 1996 Elsevier Science Limited.*

1 Introduction

Doped ceria is a solid electrolyte that is becoming increasingly attractive for use in solid oxide fuel cells (SOFC) because of its high oxygen ion conductivity, among other advantages. Whereas the routinely used but less conducting yttria-stabilized zirconia (YSZ) electrolyte has long been established in SOFC application in terms of fabrication methods, mechanical strength and chemical stability, these topics are now under investigation for the ceria-based materials.

In terms of a fabrication method, we focused on the powder preparation of doped ceria for tape casting,[1] which is a practical, industrial technique. The simple and reliable doped ceria preparation method yields active powder that is sinterable to high densities at low temperatures. High density, which was found difficult to achieve for ceria even at high temperatures until recently,[1] results in better mechanical and conduction properties.

*Present address: Ecole Polytechnique de Lausanne, Dpt. Chemistry, Institute of Physical Chemistry II, 1015 Lausanne, Switzerland.
†To whom correspondence should be addressed.

As for chemical stability in the SOFC environment, a popular solution tends towards the combination of doped ceria with a thin protective layer of the established and very stable YSZ electrolyte.[2,3] This goal in turn re-emphasizes the requirement for ceria to densify at lower temperatures than usually employed (1600°C) if, for example, cofiring of a double-layered tape-cast ceria–zirconia structure is pursued. Low temperature cofiring (<1500°C) is necessary to avoid interdiffusion. For the same reason, yttrium is used as a dopant rather than the more popular gadolinium or samarium, since the thin zirconia is yttria-doped. Furthermore, ceria is known to exhibit evaporation — or dissociation — problems at high temperature.[4]

In this study, sintering of compacts of $Ce_{0.667}Y_{0.333}O_{1.833}$ (33YDC) is investigated at temperatures between 1200 and 1600°C, with attention to densification and evaporation of the samples. A composition with a high yttrium content was purposely chosen since it supposedly densifies with greater difficulty than compositions of lower dopant concentration.[5]

Low grain boundary conductivity is also a well-known problem of ceria-based electrolytes.[6–9] It sometimes dominates the overall conductivity at low temperature, and may persist up to operation temperature (700°C). For SOFC application, the grain-boundary resistivity should ideally vanish at the projected operating temperature. The grain-boundary resistivity is reported to be a strong function of the dopant content.[9–11]

Powders in the composition range 10–33% $YO_{1.5}$ dopant concentration were synthesized and sintered to fully dense compacts in order to study the grain-boundary and total conductivity of YDC as a function of the composition. The maximum in ionic conductivity is generally believed to lie at around 5% oxygen vacancy concentration,[12] hence around 20% doping with the trivalent yttrium, but experimentally reported to range between 8

and 20% of $YO_{1.5}$ doping, depending on the temperature.[10,13–18]

Finally, an example of the correlation between density and conductivity will be given, illustrating the relevance of pursuing high density for solid electrolytes to ensure, apart from mechanical strength, the best conduction properties.

2 Experimental

The YDC powders (10–33% $YO_{1.5}$–CeO_2) were prepared by the oxalate coprecipitation method. The detailed procedure is published elsewhere.[1] In summary, it involves addition of a concentrated Ce–Y-nitrate aqueous solution (1 mol l^{-1}) under stirring to a neutral dilute oxalic acid aqueous solution (0·05 mol l^{-1}). The resulting precipitate is vacuum-filtered, washed with water and ethanol, and calcined at 700°C. This temperature was optimal to yield very compactable powder and normal shrinkage, resulting in crack-free pellets of high density. Powders of accurate composition were prepared from standardized metal nitrate solutions. The metal content of individual cerium and yttrium nitrate solutions was determined by complexometric titration with 0·01 M EDTA solution, using xylenolorange as the indicator. Direct titration could be carried out using an acetic acid/sodium acetate buffer to stabilize the solution at pH 5.

2.1 Sintering behaviour

Pellets of 33YDC, with or without prior ball milling of the powders, were pressed at 200 MPa (20 mm diameter, 1–2 mm thick) and fired at 1200–1600°C for the sintering behaviour study. Densities were measured by Archimedes' method (H_2O) and expressed as relative to the experimentally determined X-ray density [1]. Scanning electron microscopy (SEM) analysis of all samples was conducted in a Hitachi S-800 electron microscope model with an energy-dispersive X-ray (EDX) facility. With respect to the problem of ceria loss at high temperature, the metal ratio of 2:1 for Ce:Y in the $Ce_{0.667}Y_{0.333}O_{1.833}$ composition provided a convenient reference for semi-quantitative EDX analysis.

2.2 Ionic conductivity

Pellets of 10, 15, 20, 25 and 33YDC were fired fully dense at 1500°C for the conductivity study. Ionic conductivity in air at temperatures between 300 and 1000°C was measured by impedance spectroscopy in a small tubular oven. Silver electrodes of 10 mm diameter were applied by brushing silver paint symmetrically on opposite sides of the pellets using a masking technique. Four Pt wire contacts, two per electrode, were fabricated by thermocompression bonding using additional silver paint. During measurement the temperature was closely monitored by three thermocouples kept in the vicinity of the sample. The frequency range 1·3 MHz down to 5 Hz (Yokogawa Hewlett Packard 4192ALF Impedance Analyzer, Japan) or else 3 MHz down to 1 Hz (Solartron 1260, Schlumberger Electronics) was covered. Standard fitting techniques with ZARC elements[19] were used (ZView Windows 1.1, Scribner Assoc. Inc., USA) for precise grain-boundary and intragrain conductivity determination.

3 Results

3.1 Sintering behaviour of 33YDC and SEM analysis

The typical average particle size of calcined powders of all compositions (10–33YDC) was determined to be 0·7 μm. Submicrometre-sized powder is essential for ceria to sinter at normal temperatures.[1,20] The average particle size was reduced to 0·5 μm by wet milling with zirconia balls in 2-propanol (12–24 h), further improving the sinterability. Achieved relative densities as a function of the sintering temperature are displayed in Fig. 1. High density of >98% is reached at 1400°C and 1300°C for 'as-calcined' and milled powders, respectively. The sintering time at maximum temperature for all samples presented in this study was 4 h. Each pellet was placed on a zirconia or alumina fibre cloth in an open alumina crucible and fired in air, when not mentioned otherwise.

3.1.1 'As-calcined' powder

Figures 2 and 3 show surface and fracture views of 33YDC pellets fired between 1200 and 1500°C

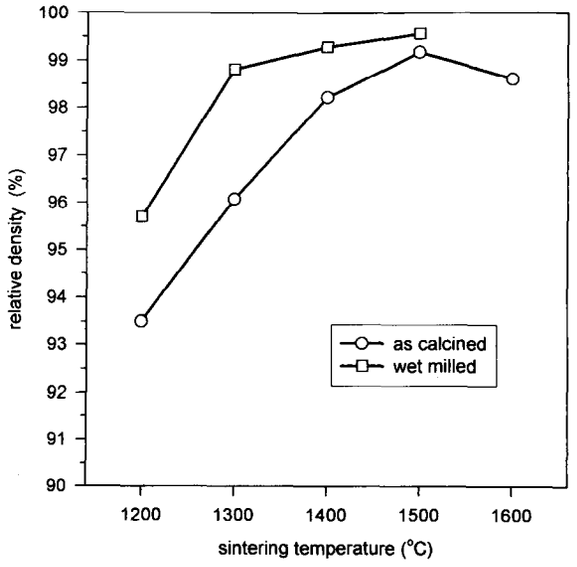

Fig. 1. Relative density of sintered 33YDC compacts (200 MPa) for various sintering temperatures (4 h), for both calcined and milled standard powder batches.

(4 h) at heating and cooling rates of 100°C h^{-1}. During sintering at 1200°C [Figs 2(a) and (b)], no grain growth has occurred yet. The particles are basically of the same size as in the starting powder. Nevertheless, 93% density was achieved at this unusually low temperature for ceria, illustrating the excellent sinterability. During sintering at 1300°C [Figs 2(c) and (d)], densification has started as clearly visible from the fracture view [Fig. 2(d)]. The grains remain very small, as evident from the surface view [Fig. 2(c)] which is identical for 'bottom' and 'top' faces of the pellets. At this temperature, closed porosity (96%) and hence impermeability is already reached. After sintering at 1400°C, the sample has fully densified [Fig. 3(c)]; grains have grown and packed together to a near dense surface [Figs 3(a) and (b)]. The top and bottom faces are not entirely identical as a minor porosity is noted at the bottom side. This phenomenon is pronounced after sintering at 1500°C, where the top face of the pellet has grown fully dense while the bottom face shows a high porosity [Figs 3(d) and (e)]. The grain growth has further increased significantly compared with firing at 1400°C. (Note that the magnification of the surface view at 1400°C is different from that of the other micrographs.)

The porosity phenomenon was identified as resulting from ceria diffusion into the underlying material. EDX measurement on the bottom face of Fig. 3(e) showed a Ce:Y ratio as low as 2:3, compared to the 2:1 ratio measured in the bulk of the sample. The porous surface layer was just a few micrometers deep, as a detailed view in Fig. 4 of the bottom and top edges of such a sample,

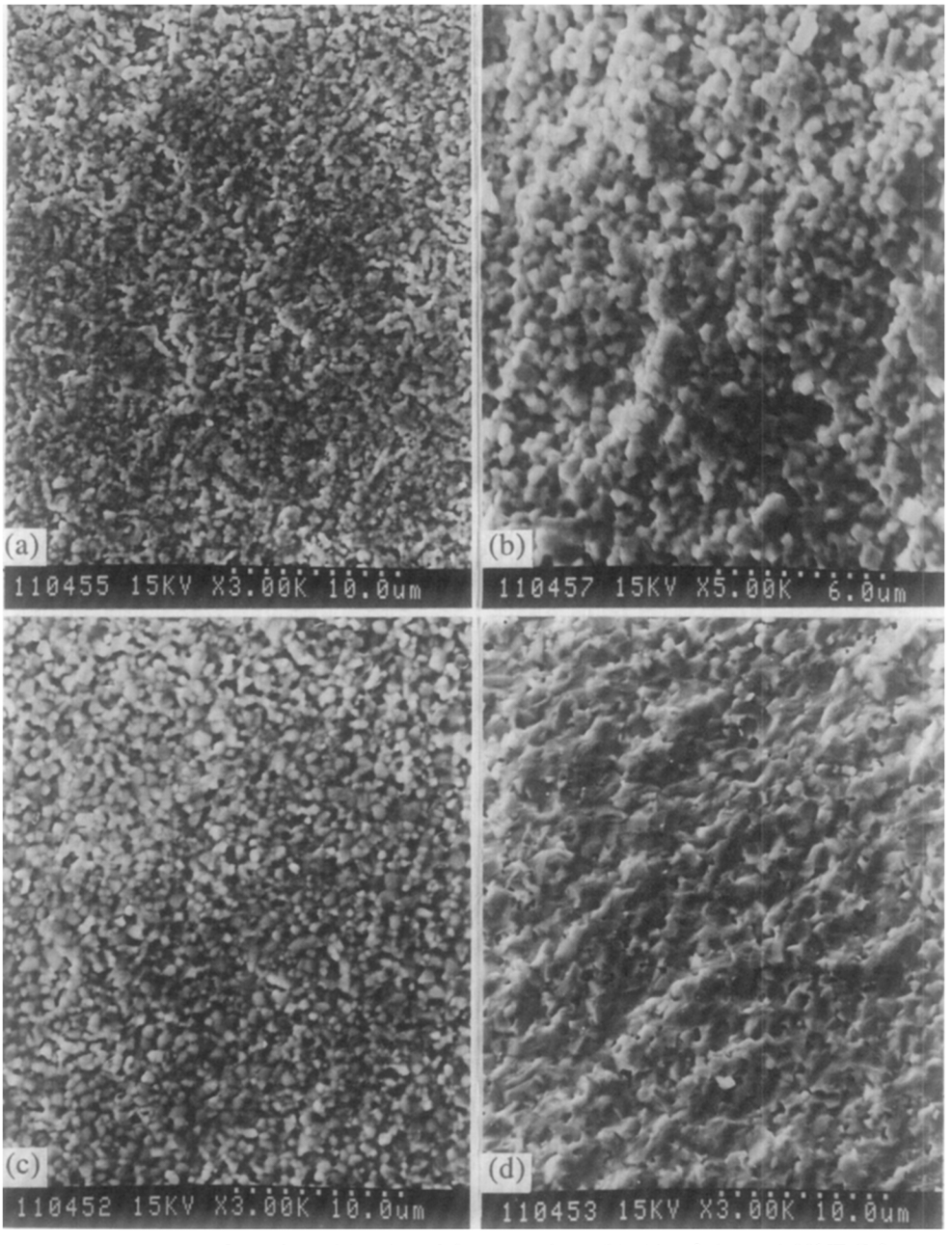

Fig. 2. SEM micrographs showing surface views (a), (c) and fracture views (b), (d) of sintered 33YDC from as-calcined powder: (a), (b) 1200°C, 4 h; (c), (d) 1300°C, 4 h.

fired at 1500°C, shows. This observation is of relevance for the application in SOFC, where reactions at the electrode/electrolyte interface play a major part in the power generation. The contact between an electrode layer with such a porous ceria-based electrolyte face might result in a large polarization loss, as the conductivity of the porous layer enriched in yttrium is considerably less than in the bulk of the sample. Therefore this loss of ceria into the substrate material during sintering at temperatures >1400°C has to be addressed.

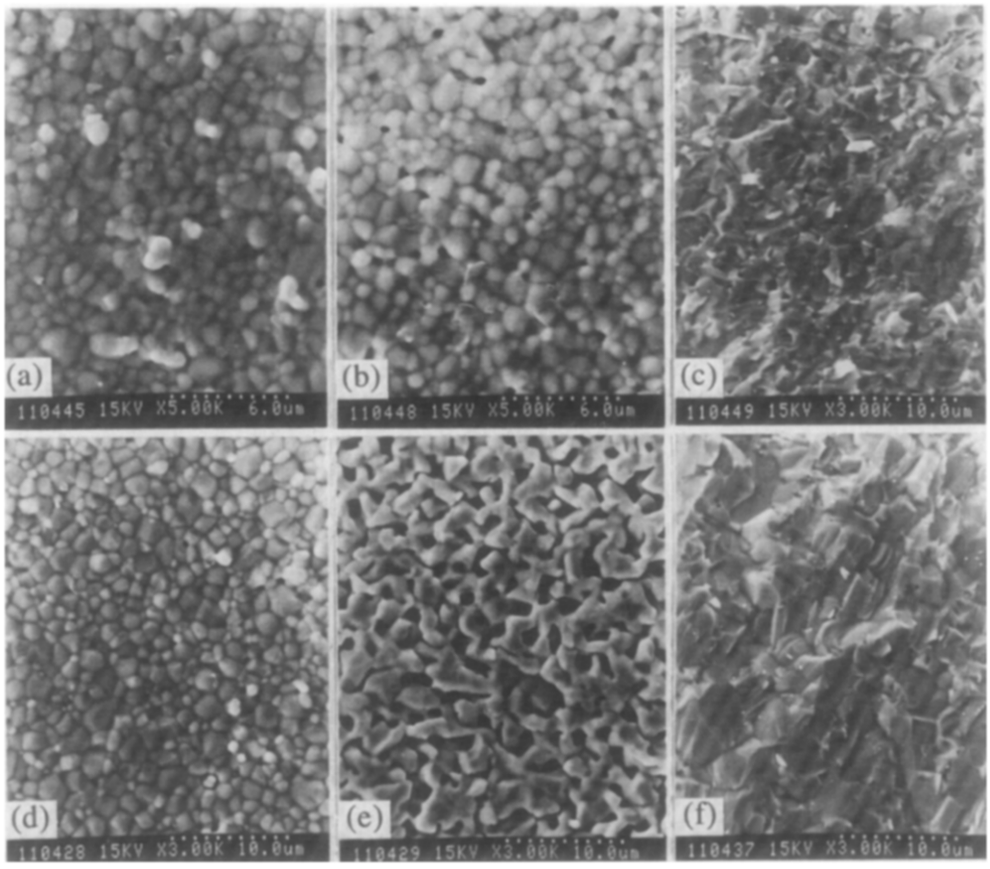

Fig. 3. SEM micrographs showing top (a), (d) and bottom (b), (e) surface views and fracture views (c), (f) of sintered 33YDC pellets from as-calcined powder: (a), (b), (c) 1400°C, 4 h; (d), (e), (f) 1500°C, 4 h.

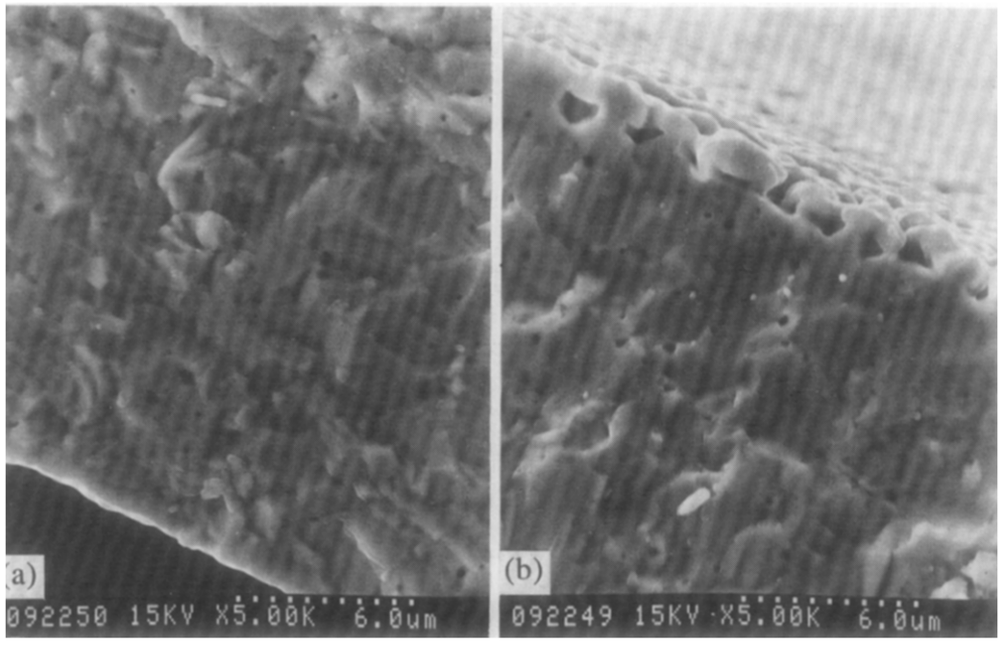

Fig. 4. SEM micrographs showing fracture views near the top surface edge (a) and near the bottom surface edge (b) of a 33YDC pellet sintered at 1500°C freely in air, without a powder bed.

3.1.2 Effect of sample embedding

As a logical solution to this problem, pellets were put on a powder bed of coarse 33YDC, entirely covered with it, and sintered at 1500°C. The SEM results of surface views of such samples are presented in Figs 5(a) and (b), which should be compared with Figs 3(d) and (e). It can be seen that the ceria loss has been entirely suppressed by this simple procedure. The bottom and top faces are equally dense.

The use of only a powder bed instead of complete embedding results in the grain growth on the 'protected', i.e. lower, face being slightly enhanced, compared with that on the upper face which was not covered with the coarse powder. This is explicitly visible from Figs 5(c) and (d) of a sample that was fired at 1500°C using a powder bed only. The grain sizes were estimated to be 1·9 and 2·2 μm for top and bottom faces, respectively.

3.1.3 Effect of heating rate

As longer times at high temperature aggravate the diffusion problem, the effect of faster heating rates, effectively shortening the residence time, was studied on samples that were not covered with additional powder on either side.

Top and bottom faces of pellets fired at 1500°C for 4 h at heating/cooling rates of 250 and 500°C h^{-1} are presented in Fig. 6, together with those for the case of a pellet fired at 100°C h^{-1} to 1500°C. It can be easily seen that faster heating rates improve densification and suppress ceria loss from the bottom

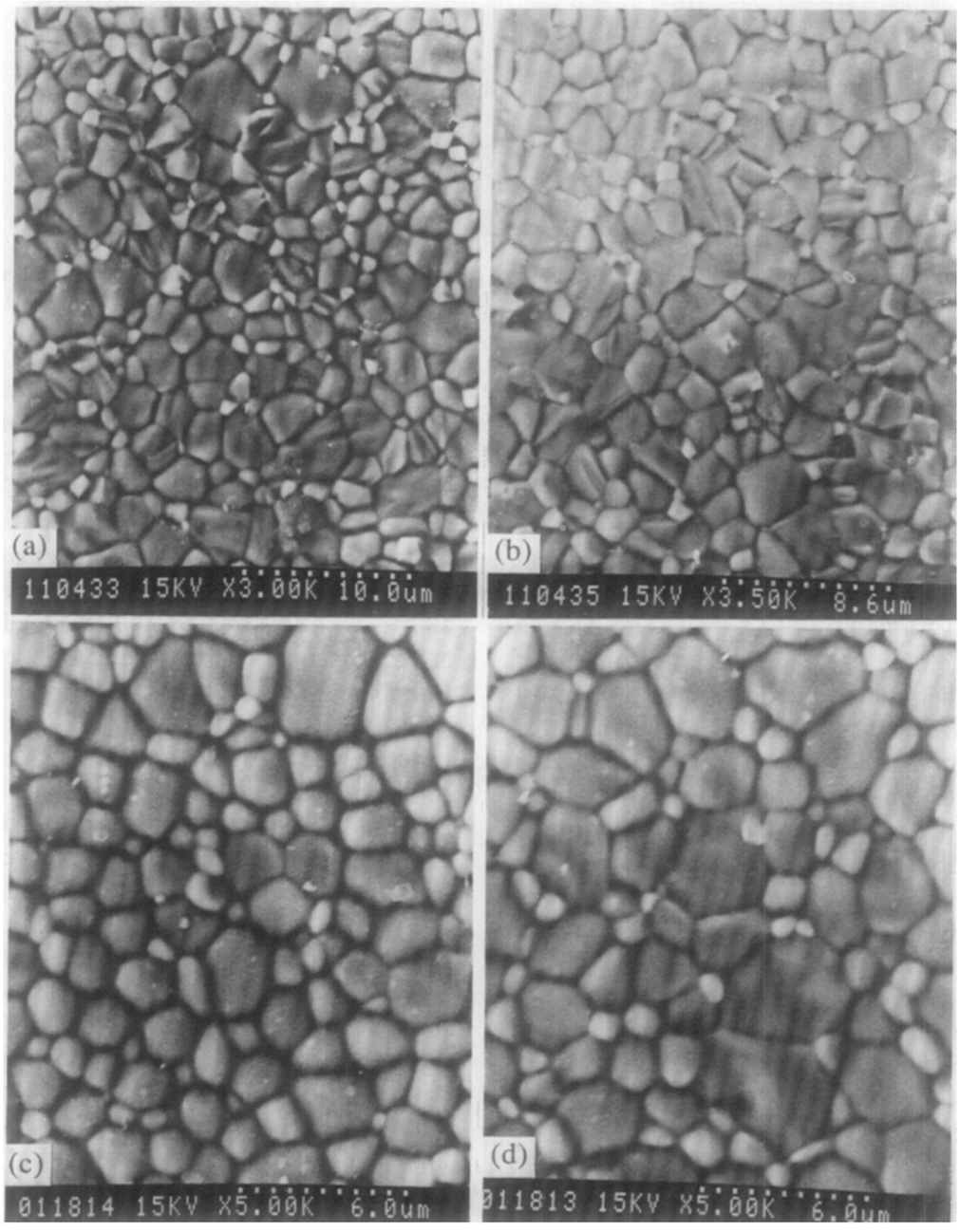

Fig. 5. SEM micrographs showing top surface views (a), (c) and bottom surface views (b), (d) of sintered 33YDC from as-calcined powder at 1500°C (4 h): (a), (b) sample entirely embedded in YDC powder; (c), (d) sample placed on a YDC powder bed only.

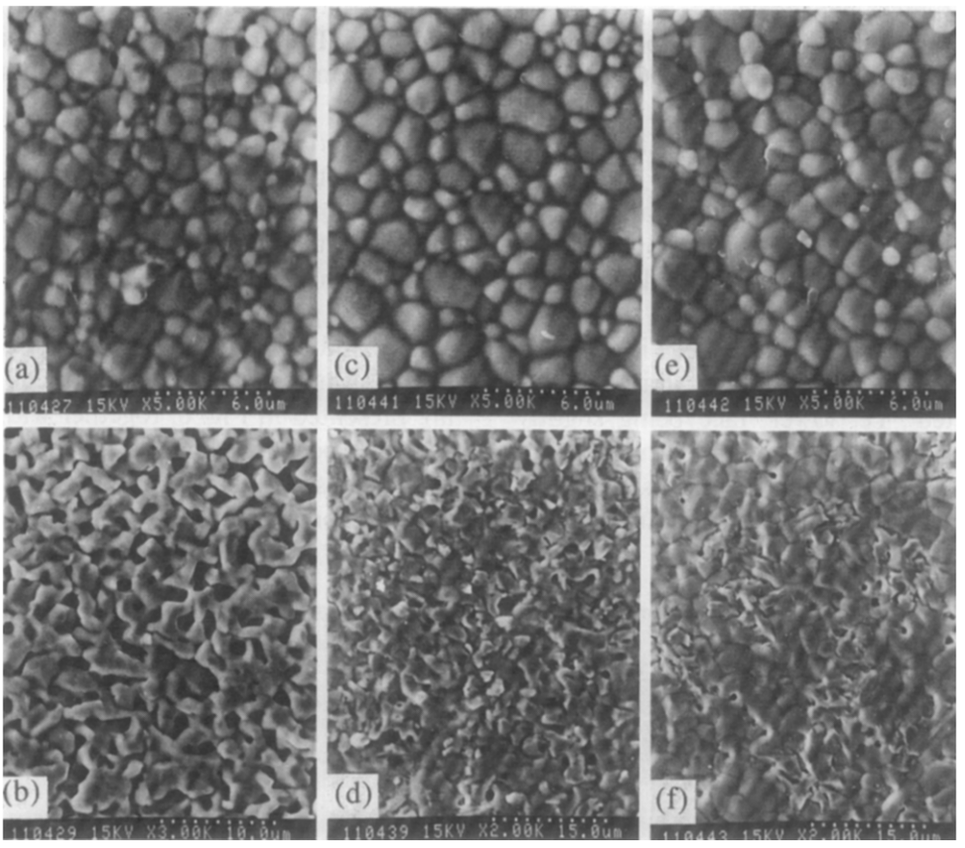

Fig. 6. SEM micrographs showing top (a), (c), (e) and bottom (b), (d), (f) surface views of sintered 33YDC pellets at 1500°C (4 h) from as-calcined powder at different heating/cooling rates: (a), (b) 100°C h^{-1}; (c), (d) 250°C h^{-1}; (e), (f) 500°C h^{-1}.

face, though not entirely. A slight increase in grain growth is observed. EDX measurements from the bottom faces of these samples gave Ce:Y ratios of 0·7 (100°C h^{-1} rate), 1·1 (250°C h^{-1}) and 1·3 (500°C h^{-1}), confirming quantitatively the suppression of ceria loss. This series of experiments demonstrates that ceria samples, in contact with other materials, can be fired safely only up to 1400°C. This should therefore be a target temperature for cofiring of ceria with other materials. Tape-cast ceria must therefore be densified at 1400°C, as we achieved and reported in another paper.[20] For isolated ceria samples, protection against ceria loss is required, e.g. by using a powder embedding or even only a powder bed, above this temperature.

3.1.4 Effect of ball milling

33YDC powder milled in 2-propanol for 12–24 h with zirconia balls in polyethylene containers, was pressed into pellets and subjected to a similar series of sintering conditions as for calcined powder. Interest was focused on the improved densification at low temperature (see Fig. 1). The samples were fired at temperatures between 1200 and 1600°C for 4 h at heating/cooling rates of 100°C h^{-1}, and without using any powder bed.

A SEM analysis is presented in Fig. 7 for top faces, bottom faces and fracture views for all sintering temperatures. At 1200°C the powder has already densified to a gas-impermeable body (Fig. 7iii), though grain size has remained small (Fig. 7i, ii). After sintering at 1300°C, the samples are near fully dense (Fig. 7vi) and grain growth was initiated (Fig. 7iv, v). In effect, the ball milling step lowers the sintering temperature by approximately 100°C with respect to the calcined powder, to achieve a similar microstructure and density. During firing at 1400°C, grain growth further increases (Fig. 7vii, viii), and at 1500°C ceria loss from the bottom face is again noted (Fig. 7xi): the Ce:Y ratio as determined by EDX was 1:1 for this sample. The problem becomes very serious at 1600°C (Fig. 7xiv), Ce:Y ratio of 0·4, where a significant increase in grain size is also observed.

In Ref. 5 it was suggested that the yttrium dopant acts as a grain growth inhibitor. In that work, the densest samples were achieved only for low $YO_{1.5}$ concentrations of 1–6%. The small grain sizes observed in this work for ceria doped with 33% of $YO_{1.5}$ seem to confirm that report. The data are plotted in Fig. 8 as estimated average grain size vs. the sintering temperature. Significant growth is not noticed until temperatures above 1500°C. However, high density could still be reached in this work at normal temperatures, despite the high yttrium content and the

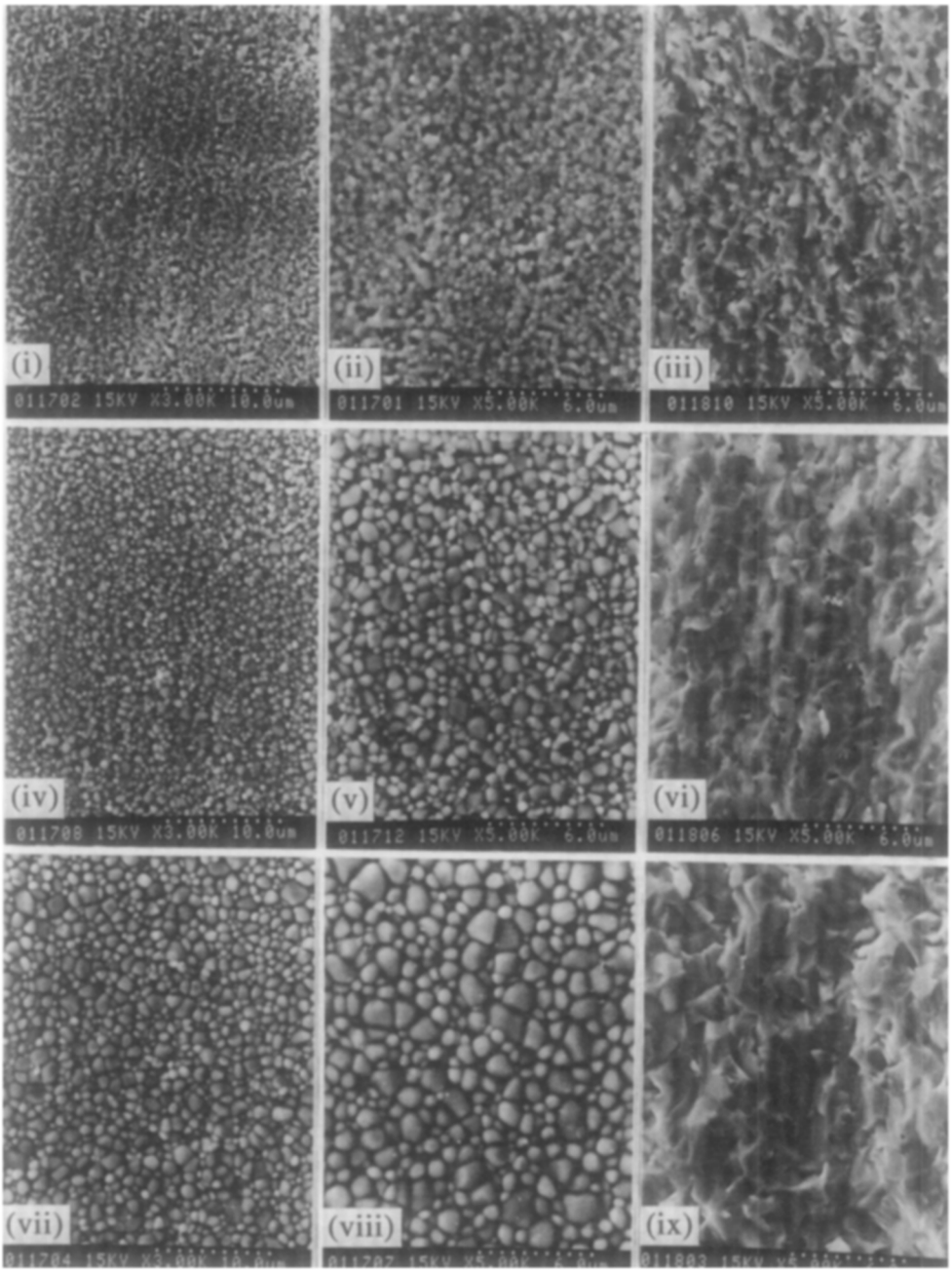

Fig. 7. SEM micrographs showing top (left column), bottom (middle column) and fracture views (right column) for sintered 33YDC pellets (4 h) from wet milled powder (2-propanol): (i)–(iii) 1200°C; (iv)–(vi) 1300°C; (vii)–(ix) 1400°C; (x)–(xii) 1500°C; (xiii)–(xv) 1600°C.

small grain size, indicating that our preparation procedure yields very active powder. This is confirmed by the fact that we were able to sinter to high density any doped ceria powder synthesized according to our procedure, independent of the composition within the range 10–33 mol% $YO_{1.5}$, or even of the dopant (Y, Gd or Sm).[21] This implies an advantage expected in terms of mechanical strength: a structure composed of fewer very much larger grains is weaker than one of many small grains, as it provides extended surfaces along which cracking can occur. Hence the densification feasibility at lower temperature presents advantages not only of practical sintering and lessening of interdiffusion, but also of better control of the mechanical properties.

3.2 Ionic conductivity

Powders of 10, 15, 20, 25 and 33 mol% $YO_{1.5}$–CeO_2 were prepared (calcination at 700°C), pressed at 200 MPa and fired at 1500°C while embedded in powder of the same composition, in order to yield fully dense samples for the conductivity measurements. A summary of the powder and compact characteristics is given in Table 1. As pointed out above, no differences in these characteristics with varying dopant content were noted, confirming a wide applicability of our powder preparation procedure.

3.2.1 Impedance spectroscopy vs. four-point method

Four-point dc measurements were carried out on sample rods in order to verify the total conductivity

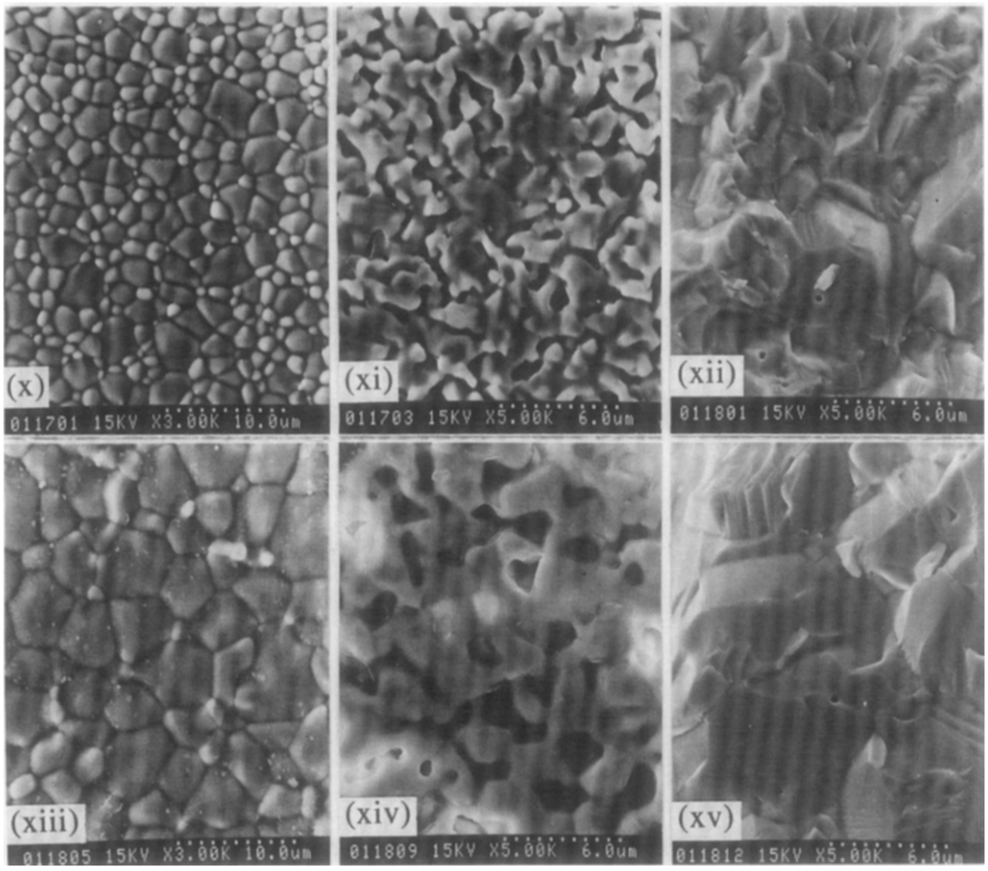

Fig. 7. Continued.

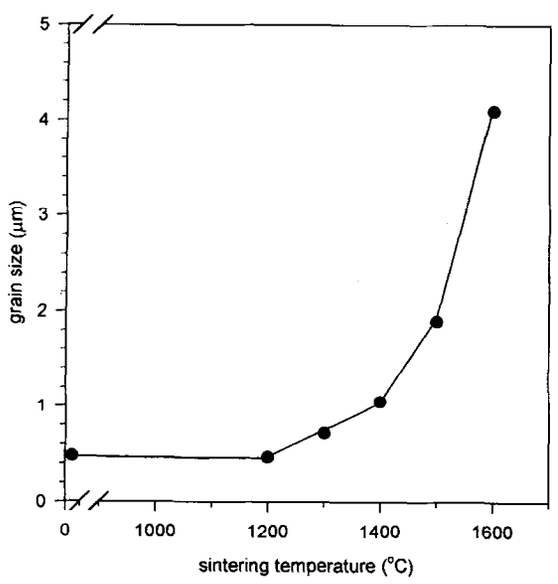

Fig. 8. Average grain size of sintered 33YDC bodies as a function of sintering temperature.

values obtained from the impedance data. Whereas this worked well for samples of high yttrium content (33YDC), a slow voltage transient phenomenon was observed after application of the current step with samples of lower yttrium content (10YDC). This phenomenon was observed and explained by previous workers.[22] Therefore impedance measurements were consistently employed for all samples, especially since grain-boundary conductivity can be decoupled from the total conductivity in the same measurement.

3.2.2 Platinum vs. silver electrodes

Silver paint electrodes (Nilaco Co., Japan) were preferred over platinum paint (TR-7905 Tanaka Kikinzoku Kogyo, Japan), since the silver electrode response was much better resolved from the grain-boundary response of the ceria electrolyte. The overlap between the latter and the platinum electrode frequency regime was rather strong, which complicated accurate determination of the total electrolyte resistance intercept. A comparison is given in Fig. 9 for a sample of 10YDC — which showed the largest grain-boundary resistance of the composition range studied — with (a) Pt electrodes and (b) Ag electrodes. Clearly, in Fig. 9(b), fitting of the second arc is more readily accomplished.

The frequencies are indicated as powers of 10 in Hz on these plots. Also, all impedance graphs shown were normalized to the same geometrical factor of 1 mm electrolyte thickness (10 mm electrode diameter), to make them comparable.

Since the grain-boundary contribution vanishes with high dopant content (≥ 25% $YO_{1.5}$), as reported before[9] and as confirmed in this work, the nature of the electrode chosen for such samples was not

Table 1. Overview of characteristic data of YDC powders of varying dopant content. d_{50} = average agglomerate size by volume, from particle-size distribution measurement in H_2O; d_{crys} = primary particle size estimated from X-ray diffraction line broadening; BET = powder surface area by N_2 adsorption; a = cubic lattice constant; ρ_{XRD} = theoretical density; ρ_{exp} = observed relative density of samples fired at 1500°C (4 h) in air

(%) $YO_{1.5}$	d_{50} (μm)	d_{crys} (nm)	BET ($m^2 g^{-1}$)	a (Å)	ρ_{XRD} ($g\ cm^{-3}$)	ρ_{exp} (%)
10	0·72	19	17·1	5·4056 ± 0·0012	6·991	99·1
15	0·71	21	20·6	5·4048 ± 0·0010	6·870	99·0
20	0·76	19	15·3	5·4016 ± 0·0107	6·753	99·4
25	0·76	23	17·1	5·4026 ± 0·0077	6·630	99·6
33	0·75	16	16·0	5·3939 ± 0·0008	6·452	99·2

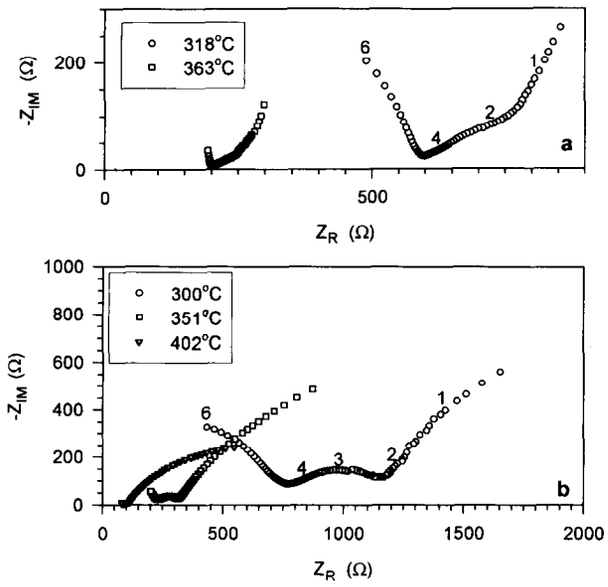

Fig. 9. Impedance diagram in air at low temperature for a 10YDC electrolyte: (a) with platinum electrodes; (b) with silver electrodes.

relevant for the measurement of the total electrolyte resistance from the real axis intercept. In the following, results on the 10, 15, 20 and 25% $YO_{1.5}$–CeO_2 material will be presented with silver electrodes, and on the 33YDC material with platinum electrodes.

3.2.3 Examples of impedance spectra

Figures 10 and 11 present two series — one at lower temperature, the other at higher temperature — of impedance responses of cells with electrolytes of the different compositions under study. Figures 9 and 10 show the results obtained with pellets of 10–33YDC in the low temperature range 300–400°C. Three arcs are distinguished, identified as bulk electrolyte semicircle (highest frequency), electrolyte grain-boundary semicircle (intermediate frequency regime) and electrode response (lowest frequency region).

Two tendencies are apparent from this series: (1) the grain boundary arc is biggest for the lower dopant concentrations, vanishing for the higher dopant regime; and (2) the total resistance (electrolyte intragrain + grain-boundary resistances) increases with increasing dopant content at this low temperature.

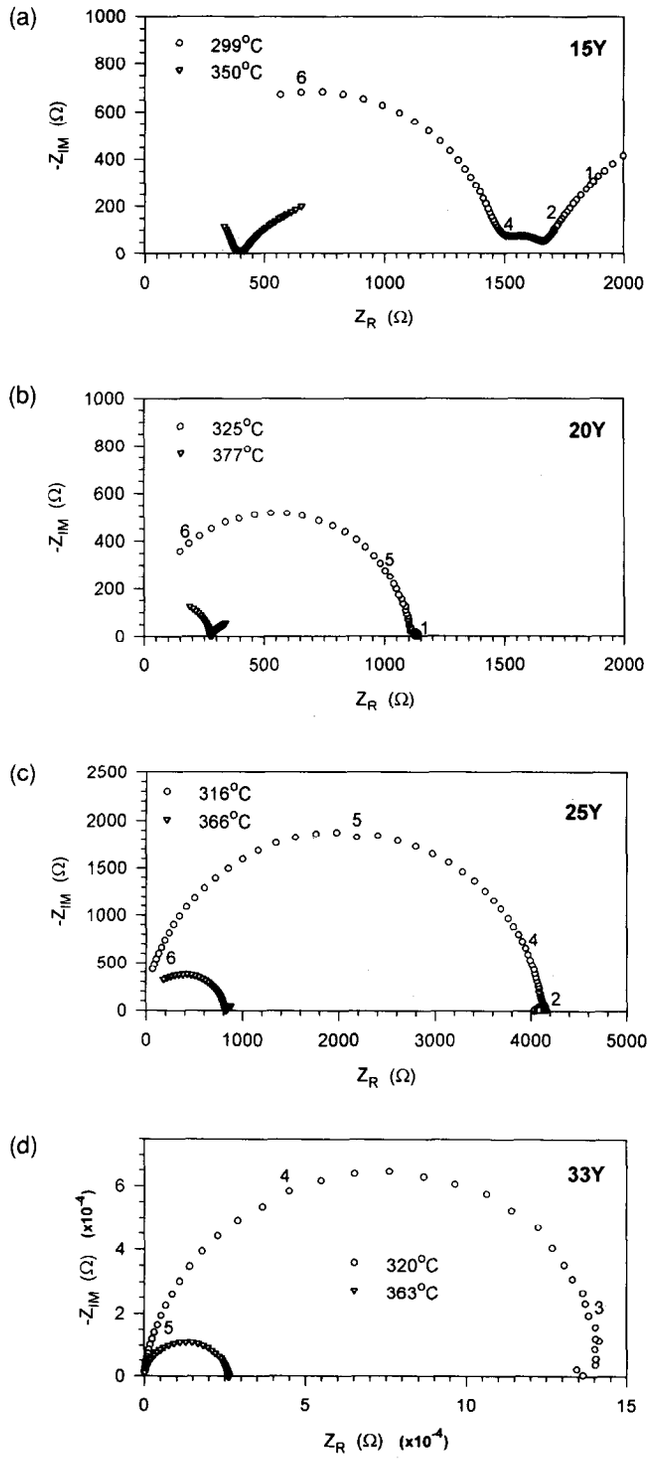

Fig. 10. Impedance diagrams in air at lower temperature (around 350°C) for different electrolytes: (a) 15YDC, (b) 20YDC, (c) 25YDC and (d) 33YDC.

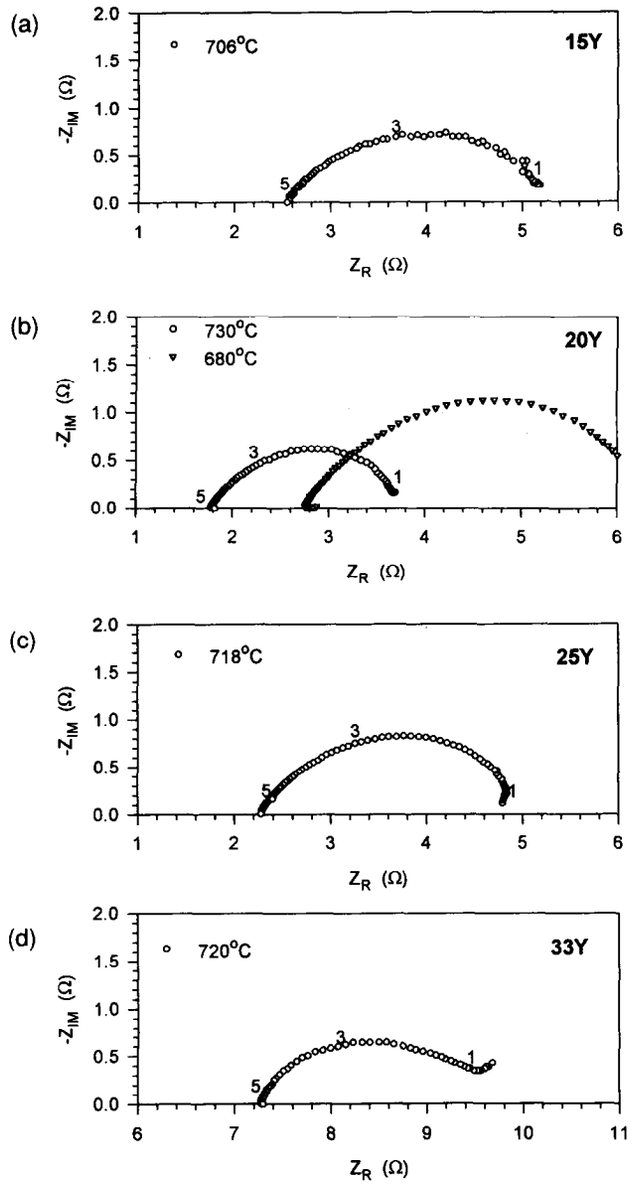

Fig. 11. Impedance diagrams in air at higher temperature (around 700°C) for different electrolytes: (a) 15YDC, (b) 20YDC, (c) 25YDC and (d) 33YDC.

Figure 11 shows the results obtained with pellets of 15–33YDC at temperatures around 700°C, a realistic SOFC operation temperature with doped ceria cells. Only the electrode response is observed at this temperature. Its shape and value are very similar and reproducible for the different pellets. The resistance is lowest for the composition 20YDC.

Data over a range of temperatures are presented in the next few graphs, elaborating more clearly the conclusions obtained from Figs 10 and 11.

Figure 12 shows the percentage of grain-boundary contribution to the total resistivity for the compositions 10–20YDC. For compositions of higher Y content no grain-boundary response was detected. The contribution is largest for the lower Y dopant concentrations at the lowest temperatures, but vanishes rapidly with increasing Y content and temperature.

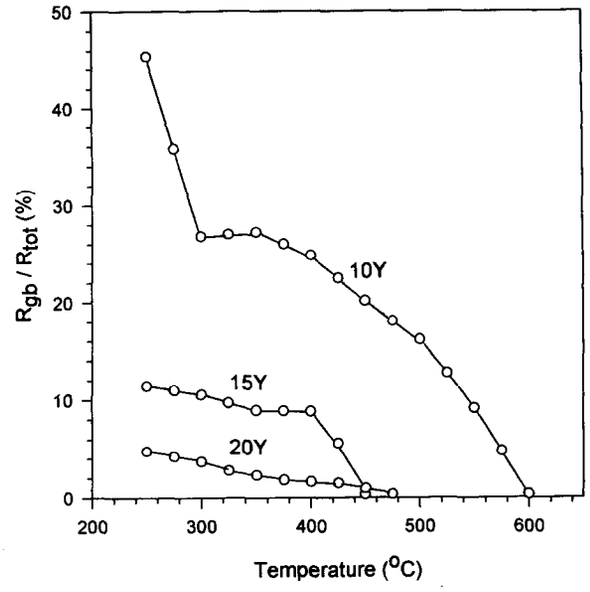

Fig. 12. Grain-boundary resistivity R_{gb} as a percentage of the total resistivity R_{tot} of YDC for different compositions, as a function of temperature.

It is to be noted that, to simplify calculations, only the geometrical electrode area and electrolyte thickness were adopted to calculate a grain-boundary 'resistivity' value from the measured resistance, rather than the real grain boundary surface and thickness which can only be estimated with difficulty. A more precise treatment using modelling has been given elsewhere.[10] Nevertheless, the relevant conclusion here is that the grain-boundary contribution becomes negligible for any Y composition studied at the projected operation temperature (>600°C). This re-illustrates the quality of our pellets and coprecipitated starting powder.

Figure 13 shows the measured total ionic conductivities of all samples over the temperature range covered as a typical Arrhenius graph. The composition giving maximum conductivity shifts with increasing temperature to one of higher Y content. This is more clearly visible from Fig. 14, where interpolated conductivity values are replotted in 100°C intervals vs. the composition. Conductivity at 300°C is a maximum at 10YDC (but may be higher at lower dopant compositions), at ~500°C at 15YDC, at 700°C at 20YDC, and at 25YDC at above 1000°C. Hence, for SOFC application at around 700°C with a doped ceria electrolyte, 20YDC is the most suitable composition in terms of ionic conductivity; this finding confirms an earlier prediction[12] and lies in the range of results of most other workers, who found maximum conductivity for the compositions 15YDC to 18YDC.[10,15,16,18] However, the conductivity difference to other compositions being small (very broad maximum in Fig. 14), properties other than conductivity, like mechanical strength, may become decisive for choosing the most suitable dopant content overall.

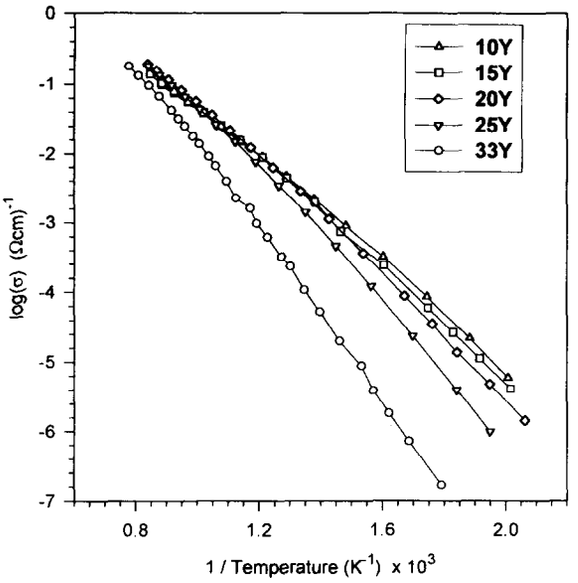

Fig. 13. Arrhenius plot over 300–1000°C of the ionic conductivity in air for YDC of the compositions used in this study.

The Arrhenius plots of Fig. 13 break up into two straight-line portions, one at low temperature (<500°C) and one at high temperature (>600°C). The activation energies for these two portions vary significantly with the Y dopant concentration, as presented in Fig. 15. Two activation energies on the same Arrhenius plot have been frequently identified before for doped ceria electrolytes.[7,10,12,23] The result of Fig. 15 differs slightly from some reports,[10,24] where the high temperature activation energy was constant in the dopant range 1–15% $YO_{1.5}$. Attractive values of 0·6–0·7 eV in the high-temperature portion of interest were observed for the samples of 10–20YDC, among the lower values observed for YDC.

The conductivity of YDC in air measured in this work is among the highest reported so far.

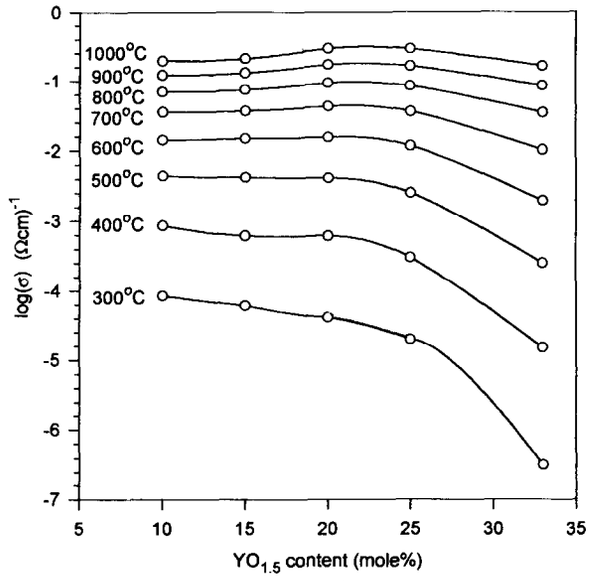

Fig. 14. Ionic conductivity of YDC in air as a function of temperature and dopant content. The composition showing maximal conductivity shifts with temperature.

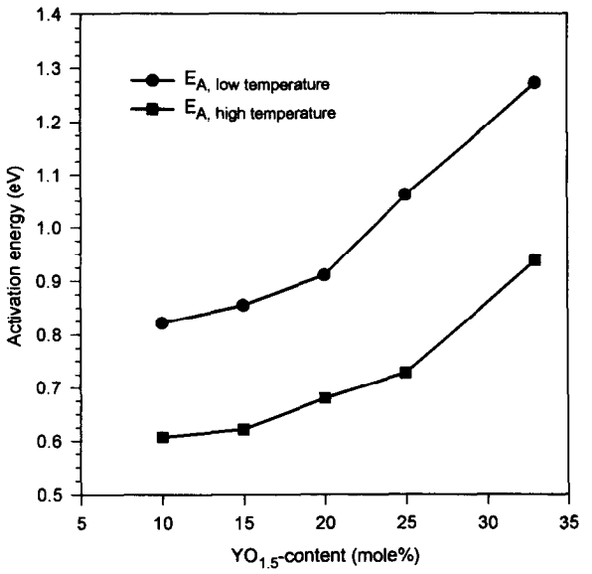

Fig. 15. Activation energies E_a for the ionic conductivity of YDC in air at low (<500°C) and high (>600°C) temperatures as a function of the dopant content, as obtained from the Arrhenius plots (Fig. 13).

Table 2 presents a comparison with literature data at 750°C, a representative operating temperature. We attribute this (1) to the optimal coprecipitation procedure giving a highly homogeneously dispersed dopant in the sample, thus yielding optimal conduction properties,[23] and (2) to the high density of the samples (99%), which has rarely been achieved in the past. A remaining porosity of a few percent or more cannot be accounted for by a simple proportional correction as is often assumed.[12,16,26] An example is given in Fig. 16, where a perfectly dense 33YDC pellet is compared in an Arrhenius plot with the ionic conductivity of a pellet of only 91%

Table 2. Ionic conductivities (σ) of YDC in air at 750°C obtained in this study, compared with literature values

Compound	σ ($S\ m^{-1}$)	*Ref.*
8·5YDC	1·2	7
20YDC	1·9	12
11YDC	2·0	9
16YDC	2·1	18
20YDC	2·2	2
15YDC	3·3	10
10YDC	3·7	25
18YDC	4·0	16
10YDC	4·7	11
20YDC	5·5	17
20YDC	6·5	This work
20GdDC	2·6	12
18GdDC	2·8	18
20GdDC	3·3	2
10GdDC	5·9	24
18GdDC	6·5	23
20GdDC	6·7	27
20SmDC	3·1	12
18SmDC	4·0	18
20SmDC	6·1	2
20SmDC	6·9	17

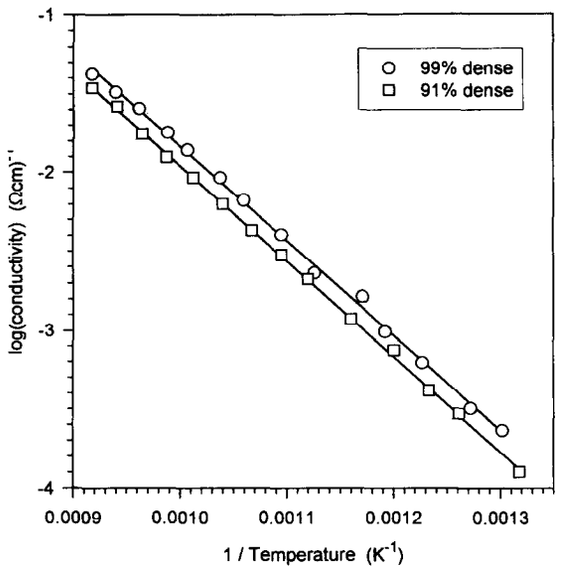

Fig. 16. Ionic conductivity (500–800°C) for 33YDC bodies of different density.

density, prepared by firing at 1100°C. On average the conductivity of the latter is worse by >25%, rather than the proportional porosity correction of ≈ 10%.

Our values for dense YDC even compare well, as Table 2 shows, with those reported for the more popular Gd- and Sm-doped cerias, generally recognised as the better conductors and hence used in preference. When abundance, price, ionic conductivity, high temperature reactivity and sinterability are considered,[21] we feel that the use of YDC compared with that of GdDC and SmDC is being neglected somewhat, more so since combination of YDC with a thin YSZ electrolyte layer should be less troublesome with respect to interdiffusion at high temperature.

4. Summary

Highly sinterable yttria-doped ceria powder was prepared, allowing densification at temperatures several hundred degrees lower than those employed in the majority of cases so far, and independent of the dopant concentration. The cerium component becomes very mobile above 1400°C, resulting, for example, in samples featuring porous surface layers if not properly protected by a powder bed. Following the high degree of densification and homogeneity of the samples, excellent conduction properties were noticed, approaching those of the more expensive Gd- and Sm-doped ceria. The conductivity maximum at 700°C, though very broad, lay at the composition around 20YDC. Lower temperature densification demonstrated in this work provides advantages in energy cost, cofiring and mechanical property control.

Acknowledgement

This work was supported by the Science and Technology Agency, Japan, which is most gratefully acknowledged.

References

1. Van herle, J., Horita, T., Kawada, T., Sakai, N., Yokokawa, H. & Dokiya, M., Yttria doped ceria: powder preparation and sintering of compacts. *J. Am. Ceram. Soc.*, submitted.
2. Eguchi, K., Setoguchi, T., Inoue, T. & Arai, H., Electrical properties of ceria-based oxides and their application to solid oxide fuel cells. *Solid State Ionics*, **52** (1992) 165–72.
3. Mehta, K., Hong, S.-J., Fue, J.-F. & Virkar, A. V., Fabrication and characterization of YSZ-coated ceria electrolytes. In *Proc. 3rd Int. Symp. on Solid Oxide Fuel Cells*. Honolulu, Hawaii, May 1993, eds. O. Yamamoto & S. C. Singhal. The Electrochemical Society, Inc., pp. 93–103.
4. Piacente, V., Bardi, G., Maluspina, L. & Desideri, A., Dissociation energy of CeO_2 and Ce_2O_2 molecules. *J. Chem. Phys.*, **59** (1973) 31–6.
5. Upadhyaya, D. P., Bhat, R., Ramanathan, S., Roy, S. K., Schubert, H. & Petzow, G., Solute effect on grain growth in ceria ceramics. *J. Eur. Ceram. Soc.*, **14** (1994) 337–41.
6. Zhen, Y. S., Milne, S. J. & Brook, R. J., Oxygen ion conduction in CeO_2 ceramics simultaneously doped with Gd_2O_3 and Y_2O_3. *Science of Ceramics*, **14** (1988) 1025–30.
7. Chiang, C. K., Bethin, J. R., Dragoo, A. L., Franklin, A. D. & Young, K. F., Inhomogeneity contribution to the electrical properties of Y-doped CeO_2 ceramics: comparison of ac and dc measurements. *J. Electrochem. Soc.*, **129** (1982) 2113–19.
8. Gerhardt, R. & Nowick, A. S., Grain-boundary effect in ceria doped with trivalent cations: I, electrical measurements. *J. Am. Ceram. Soc.*, **69** (1986) 641–6.
9. Wang, D. Y. & Nowick, A. S., The grain-boundary effect in doped ceria solid electrolytes. *J. Solid State Chem.*, **35** (1980) 325–33.
10. ElAdham, K. & Hammou, A., Etude des Propriétés electriques de solutions solides à base de dioxyde de cérium. *J. Chim. Phys.*, **79** (1982) 633–44.
11. Subbarao, E. C. & Maiti, H. S., Solid electrolytes with oxygen ion conduction. *Solid State Ionics*, **11** (1984) 317–38.
12. Dirstine, R. T., Blumenthal, R. N. & Kuech, T. F., Ionic conductivity of calcia, yttria, and rare-earth doped cerium dioxide. *J. Electrochem. Soc.*, **126** (1979) 264–9.
13. Wang, D. Y., Park, D. S., Griffith, J. & Nowick, A. S., Oxygen ion conductivity and defect interactions in yttria-doped ceria. *Solid State Ionics*, **2** (1981) 95–105.
14. Sarkar, P. & Nicholson, P. S., Ac conductivity and conductivity relaxation studies in the CeO_2–Y_2O_3 system. *Solid State Ionics*, **21** (1986) 49–53.
15. Catlow, C. R. A., Transport in doped fluorite oxides. *Solid State Ionics*, **12** (1984) 67–73.
16. Pascual, C., Jurado, J. R., Arroyo, G. F., Del Olmo, L., Moure, C. & Duran, P., Electrical conductivity of solid solutions in the systems CeO_2–CaO and CeO_2–Ln_2O_3 (Ln = La, Nd, Sm, Gd, Er, Y). *Science of Ceramics*, **12** (1984) 729–34.
17. Yahiro, H., Baba, Y., Eguchi, K. & Arai, H., High temperature fuel cell with ceria-yttria solid electrolyte. *J. Electrochem. Soc.* **135** (1988) 2077–81.
18. Balazs, G. B. & Glass, R. S., Ac impedance studies of rare earth oxides doped ceria. *Solid State Ionics*, **76** (1995) 155–62.
19. MacDonald, J. R., *Impedance Spectroscopy*. John Wiley & Sons, New York, 1987, pp. 90–5.

20. Van herle, J., Horita, T., Kawada, T., Sakai, N. Yokokawa H. & Dokiya, M., Yttria doped ceria: tape casting. *J. Am. Ceram. Soc.*, submitted.
21. Van herle, J., Horita, T., Kawada, T., Sakai, N., Yokokawa, H. & Dokiya, M., Low temperature fabrication of (Gd,Sm,Y)-doped ceria electrolyte. *Solid State Ionics*, submitted.
22. Chiang, C. K., Dragoo, A. L. & Franklin, A. D., Slow transient phenomenon in Y-doped CeO_2. In *Fast Ion Transport in Solids*, eds. P. Vashishta, J. Mundy & G. Shenoy. North Holland Elsevier, 1979, pp. 661–3.
23. Riess, I., Braunshtein, D. & Tannhauser, D. S., Density and ionic conductivity of sintered $(CeO_2)_{0.82}(GdO_{1.5})_{0.18}$. *J. Am. Ceram. Soc.*, **64** (1981) 479–85.
24. Hohnke, D. K., Ionic conduction in doped oxides with the fluorite structure. *Solid State Ionics*, **5** (1981) 531–4.
25. Mogensen, M., Lindegaard, T., Hansen, U. R. & Mogensen, G., Physical properties of mixed conductor solid oxide fuel cell anodes of doped CeO_2. *J. Electrochem. Soc.*, **141** (1994) 2122–8.
26. Tuller, H. L. & Nowick, A. S., Ionic conductivity of doped cerium dioxide. In *Proc. Conf. on High Temperature Solid Oxide Electrolytes*, August 1983, ed. F. Salzano. Brookhaven Nat. Lab. Assoc. Univ. Inc., Upton, NY, pp. 177–85.
27. Kudo, T. & Obayashi, H., Oxygen ion conduction of the fluorite-type $Ce_{1-x}Ln_xO_{2-x/2}$ (Ln = lanthanide). *J. Electrochem. Soc.*, **122** (1975) 142–7.